Structural dynamic reliability analysis of super large-scale lattice domes during earthquakes using the stochastic finite element method

Huidong Zhang[1,2*], Ning An[1,2], Xinqun Zhu[3]

[1]School of Civil Engineering, Tianjin Chengjian University, Tianjin 300384, China

[2]Tianjin Key Laboratory of Civil Buildings Protection and Reinforcement, Tianjin 300384, China

[3]School of Civil and Environmental Engineering, University of Technology Sydney, NSW 2007, Australia

[*]Corresponding author: Huidong Zhang, School of Civil Engineering, Tianjin Chengjian University, Tianjin 300384, China; E-mail: zhhuidong@126.com

Abstract: For large-scale dome structures subjected to earthquake ground motions, the need for accurate and efficient approaches that account for uncertainties in design, material properties, loads, damping, and manufacturing processes has grown significantly. In uncertainty analyses, the theory of probability, uncertainty quantification, and reliability analysis approaches are commonly used. However, because of computing efficiency and capability, the space scale of dome structures is severely limited. As a result, the complex dynamic reliability issues that super large-scale dome structures face during earthquakes have not been thoroughly investigated. The uncertainties of the dynamic demands of a super large-scale lattice dome with multiple variables are quantified using a novel stochastic finite element method (SFEM) with nonlinear time-history analysis developed in this paper. The dynamic reliability problems are investigated using the efficient Latin Hypercube sampling (LHS) technique to reduce the number of repeated time-consuming calculations. To improve the efficiency and accuracy of the analysis, an optimization approach based on the genetic algorithm (GA) is used to obtain the probability of structural failure and the reliability index. The results show that these methods are efficient for super large-scale structures. A sensitivity analysis based on variable randomness is conducted to further evaluate the effects of unknown variables on structural performance using various evaluation methods. The stochastic finite element modelling is incorporated into the nonlinear dynamic time-history analysis of larger-scale systems to address engineering reliability issues.

Key words: super large-scale dome; uncertainty; Latin Hypercube sampling; genetic algorithm; seismic performance

1. Introduction

The core of performance-based seismic engineering (PBEE) is to accurately predict structural seismic performance [1]. Nevertheless, it is important to note that almost all of the parameters in practical structures have uncertain characteristics due to aleatory randomness and epistemic errors. These uncertain parameters are divided into two categories: the low level and the high level uncertainties [2]. The low-level uncertainties are concerned with the stress-strain relationships of the materials or the force-deformation relationships of the members, while the high-level uncertainties are concerned with structural systems such as the structural shape, structural imperfections, structural damping characteristics, and loads. The estimation of structural seismic performance is complicated by these uncertain variables.

Several previous studies [3-5] have shown that when various sources of uncertainty are considered, the accuracy of structural performance assessments can be significantly improved in the nonlinear seismic response of structures. There are a few methods to address the effects of uncertain sources on structures. In the traditional assessment method known as load and resistance factor design (LRFD), various uncertainties in a structure are taken into account by reducing resistance parameters and

magnifying loadings to ensure structural safety. This type of evaluation method is usually deterministic in nature. Deterministic methods have been used for structural studies for a long time. Although the deterministic strategy can ensure structural safety with high reliability, it is imprecise and cannot disclose the true seismic performance of structures because it cannot explicitly model uncertainties of variables.

Dealing with uncertainty by introducing probability theory, which can describe the properties of variables [3], is an important and advanced analysis method. Researchers and engineers have been paying closer attention to structural probabilistic analysis (SPA) in recent years. The SPA is able to evaluate structural seismic performance with greater robustness, higher precision, and less conservative estimates than conventional evaluation methods [2]. Furthermore, by determining whether the limit state function is exceeded, probabilistic structural analysis can evaluate the probability of structural failure. As a result, deterministic evaluation methods based on the LRFD strategy can be greatly improved.

As early as more than three decades ago, Cruse and Wu et al. [6] reported an advanced algorithm for simulating the probabilistic distribution of structural responses due to statistical uncertainties in loads, geometry, material properties and boundary conditions. Uncertainty analysis (UA) and probabilistic analysis for the evaluation of structural performance have gained more attention in the last two decades [7]. Matthies et al. [8] addressed the new techniques in stochastic modelling in depth for uncertain variables involved in structural analysis using stochastic finite element methods. Taking into account the variability of geometric shapes, Haukaas and Scott [9] suggested a unified and systematic treatment method for variations of the nodal coordinates and global shape parameters of inelastic frame structures. Zhang et al. [10, 11] developed an interval Monte Carlo method that combined a simulation process with interval analysis and predicted the probabilities of failure of planar steel structures. Considering uncertainties in both material properties and static loads, Le and Xue [12] calculated the occurrence probabilities of various damage degrees of planar frame structures. Liel and Haselton [13] used the response surface and first-order second moment (FOSM) methods to perform detailed probabilistic collapse risk assessments of frame buildings, taking into account uncertain parameters such as structural component strength, stiffness, deformability, and cyclic deterioration. Other typical studies of probabilistic analyses of structures with variables have been reported [14-17].

In SPA, the sampling technique plays an important role. For probabilistic evaluations, direct Monte Carlo sampling is not efficient, particularly when the failure probability is low. However, due to its universal applicability, it is only used as a last resort if no other alternatives are available. To improve the efficiency of probabilistic structural analysis, several probabilistic methods and algorithms have been developed in recent years. Zhang et al. [18] introduced a new structural reliability quantification method based on random variables, and the reliability of simple structures was evaluated using the developed probability-uncertainty hybrid model. Jiang et al. [19] proposed a hybrid uncertain model-based reliability analysis methodology for uncertain structures. Králik [20] used Monte Carlo (MC), importance sampling (IS), Latin hypercube sampling (LHS), and response surface methods to conduct probabilistic analyses for a high-rise building in static situations and discussed the advantages and drawbacks of these methods. Hariri-Ardebilia and Sudret [21] applied the polynomial chaos expansion (PCE) to the uncertainty quantification of dam structures with variables, and it was found that the PCE is an effective technique for uncertainty quantification in concrete dams. Wang et al. [22] proposed an extremum kriging method (EKM) with a multi-population genetic algorithm (MPGA) to improve the computational efficiency of dynamic probabilistic analysis for complex structures.

Additionally, Cui and Sheng [23] presented a genetic algorithm (GA) method that was integrated into the displacement finite element method for probabilistic failure analysis of geotechnical structures, indicating that GA offers new opportunities for probabilistic finite element analysis of engineering structures. To keep the computational effort acceptable in reliability analysis, adaptive techniques based on artificial neural networks (ANNs) were proposed using surrogate models [24, 25]. In essence, the above methods are approximate and data-driven, only the input-output behaviour is important and the system is assumed to be a black-box structure; however, the number of samples is also important since a small number of samples cannot completely reflect the properties of the structure system. This problem can now be solved with a large sampling size due to the development of high-performance computing. Evidently, structural reliability analysis still relies on probabilistic estimates with a sufficient sample size. Furthermore, the studies described above are more focused on the global sensitivity analysis of structural systems, and these methods have drawbacks in engineering applications when considering the randomness at the local level.

Although nonlinear time-history analysis (NTHA) has been widely used for estimating dynamic demands and structural seismic performance in PBEE frames and the use of SPA methods in combination with NTHA may enhance the evaluation of structural seismic performance and ensure structural safety, most researchers consider that performing dynamic probabilistic analysis is extremely time-consuming. As a result, ″static equivalent″ methods for dynamic analysis have been developed to reduce the computational burden caused by structural complexity. However, for real-world structures, combining SPA with NTHA is important because it accurately explains real-world structural performance during earthquakes. Furthermore, probabilistic structural dynamics provides unparalleled tools for evaluating uncertainties in structural design, and it may eventually replace traditional deterministic analysis approaches.

Structural reliability research is currently emerging in the areas of structural dynamic reliability, structural fatigue reliability, structural fracture reliability, structural system reliability, structural optimization design based on reliability, and generalized reliability with fuzzy factors [26, 27]. However, current research on structural reliability is based on simple structures and component levels, and the dynamic reliability for complex full-scale structures during earthquakes has not been extensively investigated.

In this paper, a stochastic finite element method (SFEM) is developed using the probabilistic principle and the finite element method to understand the performance of structures with variables. The structural dynamic reliability analysis of a super large-scale lattice dome is carried out based on the SFEM. Highly efficient LHS methodology, parallel computing, and genetic algorithms (GAs) are implemented in dynamic reliability analyses to improve computational efficiency and accuracy. Finally, different evaluation indices are used to measure the effects of variables on structure performance.

2. Uncertainty modelling

2.1 Quantification of uncertainty

Quantifications of uncertainties in engineering structures are usually expressed as a probability distribution, which indicates how likely each possible value is. The most common form of distribution in engineering is the normal distribution is, as shown in Fig. 1. The value range of variable X can be expressed by Eq. (1),

$$X \in \{\mu - c\sigma, \mu + c\sigma\} \tag{1}$$

where μ and σ represent the mean and standard deviation of the variable X, respectively, and c is the scale factor of σ. Low probability events are classified as those with a probability of less than 5%,

according to hypothesis testing theory. According to the "3-sigma" principle, the odds of variable X being the intervals of $\{\mu-3\sigma,\mu+3\sigma\}$ and $\{\mu-2\sigma,\mu+2\sigma\}$ are less than 3‰ and 5%, respectively. Since it is considered that events with a probability of 3‰ do not occur in realistic structural engineering, the interval $\{\mu-3\sigma,\mu+3\sigma\}$ can be considered the potential interval of the random variable X. The true interval for engineering issues can be even smaller due to engineering quality control and assurance. In probabilistic models, the ranges of the potential values of the variables should be carefully considered. Truncated distribution functions are used to model the distribution characteristics of the variables in this paper.

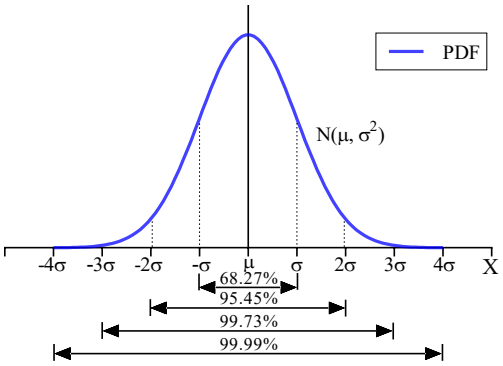

Fig. 1 Probability density function (PDF) of the normal distribution

2.2 Uncertainty modelling methods

The main sources of uncertainty for large-scale domes have been established [17], which includes the elastic modulus E, yielding strength f_y, and strain-hardening ratio b at the material level and several uncertain parameters at the structural level, such as various structural shape imperfections, the wall-thickness of member t_w, the structural damping ratio ξ, and internal loads m. External excitation is a special form of uncertainty source. Previously, probabilistic analysis was conducted on structures with just a few uncertain parameters; however, it has not been widely applied to structures with all of the variables listed above.

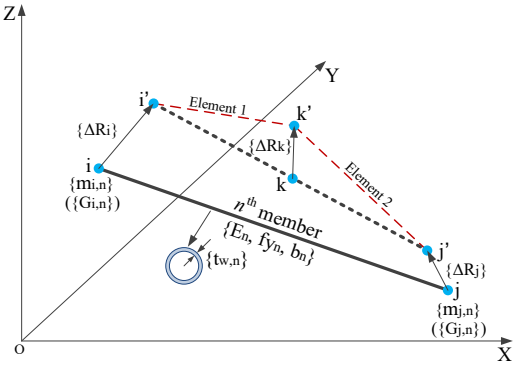

Fig. 2 Uncertainty modelling

Fig. 2 shows the modelling details for the uncertainties of the n^{th} member in a structure, where $\{\Delta R_{i,j}\}$ is the node error vector of the member. The literature [17] offers more modelling information for this uncertain source, and this paper follows the simulation method suggested in this reference. The coordinate error vector $\{\Delta R_k\}=\{\Delta x_k+\Delta y_k+\Delta z_k\}$ of the span-middle node k is used to model the initial imperfection of a member. However, unlike previous modelling methods, this paper assigns the values of each low-level variable and the wall-thickness parameter to each member, making each member unique. According to equivalence, internal loads are treated as an uncertain node mass m, resulting in an uncertain static node load. The entire structure is assigned an uncertain damping ratio,

and the uncertainty of the external excitations is realized by taking into account the uncertainties of the three-directional amplitudes of the excitations.

The classical deterministic finite element method is extended to SFEM in this paper based on the above modelling technologies for uncertainties. SFEM has received considerable attention because of the tremendous growth of computing capacity over the last 20 years. Direct modelling of structures with multiple variables is a major challenge in SFEM. Most commercial finite element programs currently available cannot perform finite element analysis of stochastic structures in the true sense, and what they can do is more analogous to a global sensitivity analysis of structures. However, the methods and compiled program provided in this paper can solve this problem, and the study of stochastic structures with variables can be realized, including the external time-history loads.

3. Structural reliability estimation

3.1 Structural reliability

Structural reliability is a quantitative index that is used as a probabilistic measure of structural safety and is currently a popular design philosophy. When loads and resistances are explicit and have their own independent function, the probability of failure can generally be expressed as follows [6],

$$P_f = P(g(X) < 0) = \int_{-\infty}^{\infty} f_E(x)\, \Phi_R(x)\, dx = \int_{-\infty}^{\infty} \Phi_E(x)\, f_R(x) dx \tag{2}$$

where P_f is the probability of failure, $g(X)$ is the failure function, $f_E(x)$ and $f_R(x)$ are the probability density functions of load effects and resistance, respectively, and $\Phi_E(x)$ and $\Phi_R(x)$ are the corresponding cumulative distribution functions. The integral of Eq. (2) can only be solved analytically for simple cases; for complicated cases, the function expressions are not actually clear, and analytical solutions are difficult to obtain. The probability of failure can be determined using a sampling simulation.

The reliability index β is widely used in engineering to define structural safety. The failure probability can be used to measure the reliability index β by a normally distributed limit state function,

$$\beta = -\Phi^{-1}(P_f) \tag{3}$$

where Φ is the standardized normal cumulative distribution function.

3.2 Sampling method

In a Monte Carlo simulation, Latin hypercube sampling (LHS) is a variance reduction technique for generating random samples of parameter values. It can save computing time in Monte Carlo simulations by significantly reducing the number of runs needed to obtain a fairly accurate result. It has been reported that this method can reduce the computing time by up to 50% compared to regular Monte Carlo sampling [20]. Furthermore, by using a simple sampling method to generate random samples, the data may be over-aggregated, while the LHS method can avoid this case. The standard LHS steps are as follows [28],

- The number of generated samples, N, is defined first in LHS.
- According to the uniform distribution, the interval [0, 1] is divided into N equal small intervals, and a random value $p_{i,j}$ is generated in each interval of $[i/N, (i+1)/N]$, as shown in Fig. 3. Each value represents the cumulative probability for the stochastic value of a variable. This value is equal to $(\delta + i)/N$, where δ is a random value with a uniform distribution. δ and i are in the ranges of $[0, 1]$ and $[0, N-1]$, respectively.
- The N random values are sorted at random.
- Using the above N random values, the inverse function of the unique probability distribution function $F^{-1}(\cdot)$ is used to generate N values of the variable.

The LHS in this paper can better explain the distribution characteristics of variables and improve modelling and computational simulation. The random value p_i is set to $i/(N-1)$, where i is within the range of $[0,\ (N-1)]$. The maximum, minimum, and other values of the variable can be obtained in this manner. Fig. 4 provides a comparison of the above two methods for probability density functions using a sample size of 320. The current method fully fits the real curve and presents the probability characteristics of the variable, while the conventional method cannot obtain values corresponding to a small probability density.

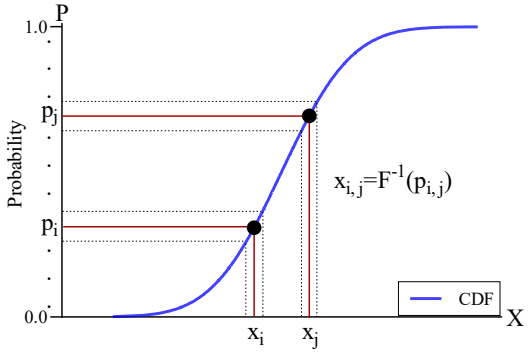

Fig. 3 LHS method

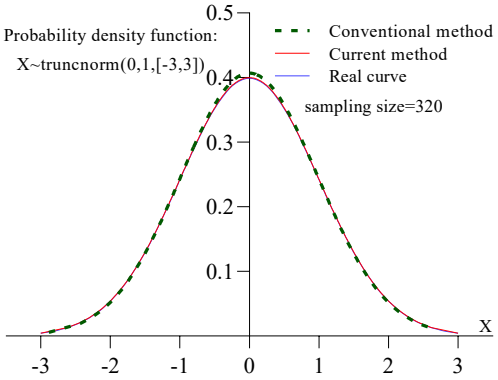

Fig. 4 A comparison of two methods

3.3 Advanced optimization methods for PDFs of structural demands

For practical engineering problems, sufficient sampling structures are not always usable, and obtaining them can be difficult and time-consuming with a large sample size. The sampling method must be effective enough under the condition of a finite sample size, as described in Section 3.2 and illustrated in Fig. 4, and the LHS method completely explains the probability properties of variables with a small sampling size. However, numerical fitting techniques with high precision are needed to optimize the PDF and cumulative probability function (CDF) based on discrete demand values obtained from a finite sample size.

The generalized extreme value (GEV) distribution, which is commonly used in ecology, hydrology, engineering, climate, and finance [29, 30], is a well-accepted optimizing model for PDFs and CDFs. The GEV distribution is defined as [31],

$$f(x) = \frac{1}{\delta} t(x)^{k+1} exp\ (-t(x)) \tag{4}$$

where

$$t(x) = \begin{cases} (1 + k\frac{x-mu}{\delta})^{-1/k} & if\ k \neq 0 \\ exp\ (-\frac{x-mu}{\delta}) & if\ k = 0 \end{cases} \tag{5}$$

and $k,\ mu,\ \delta$ are the shape, location, and scale parameters, respectively, and $\left(1 + k\frac{x-mu}{\delta}\right)$ must be greater than zero. The cumulative distribution function is defined as follows [31]:

$$F(x) = exp(-t(x)) \tag{6}$$

The genetic algorithm (GA) is considered in this paper to carry out the optimization for the obtained PDFs using the GEV probability model to further improve the optimization accuracy. GA is a machine learning search technique inspired by the process of natural selection that belongs to the larger class of evolutionary algorithms (EAs). GAs rely on biologically inspired operators such as mutation, crossover and selection to produce high-quality solutions to optimization and search problems. Further

information about GA can be found in the literature [32]. The steps for GA to improve PDFs are as follows,

•The discrete values of the structural demands are obtained through dynamic analyses of the sampling structures using SFEM.

•The GEV model is used to fit the PDF based on the calculated histogram shape of the structural demand.

•A fitness function is designed to optimize the unknown parameters in the GEV model.

The selection of the fitness function in GA has a direct effect on the convergence rate of GA; as a result, the fitness function should be as simple as possible to reduce calculation complexity. The fitness function for the PDF in this paper is designed as follows,

$$\Delta y = (\sum_{i=1}^{n} abs(y_{f,i} - y_{r,i}))/n \tag{7}$$

where Δy is the value of the fitness function, $y_{f,i}$ and $y_{r,i}$ are the i^{th} fitting value and real value, respectively, and n is the number of data points to fit. The constraint function is written as follows,

$$1 + k\frac{x-mu}{\delta} > 0 \tag{8}$$

The values of the essential parameters in the GA are summarized and listed in Table 1 based on experience from a wide body of literature. The unknown variables in Eqs. (4) and (5) are optimized in this paper based on the results.

Table 1 Values of important parameters in the GA.

Parameter	PopulationSize	CrossoverFraction	MigrationFraction	Generations	TolFun
Common case	[20, 100]	[0.4, 0.99]	[1e-4, 0.1]	[100, 500]	1e-50
Current work	[40, 60]	[0.7, 0.8]	[0.04, 0.09]	[200, 400]	1e-50

The predictive squared correlation coefficient (Q^2) is used as an evaluation criterion to compare the fitting performance of different methods. The expression for Q^2 is as follows [33],

$$Q^2 = 1 - \frac{\sum_{i=1}^{i=n}(y_{r,i}-y_{f,i})^2}{\sum_{i=1}^{i=n}(y_{r,i}-\bar{y}_{r,i})^2} \tag{9}$$

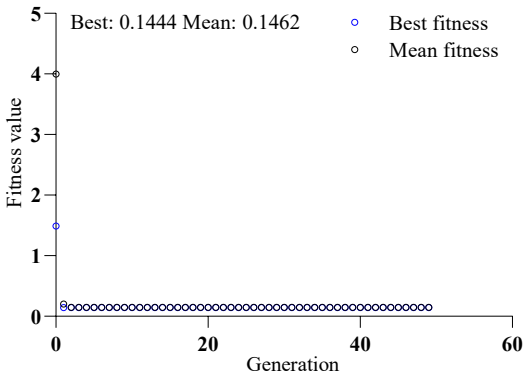

Fig. 1 Fitness value in a typical GA optimization

$y_{f,i}$ should be equal to $y_{r,i}$ for perfect fitting in the PDF. The value of Q^2 varies from -1 to 1, and the higher the value of Q^2, the better the fitting effectiveness. Models with a value greater than 0.8 have a high goodness-of-fit. As shown in Fig. 5, in typical GA optimization for a PDF, the fitness tends to improve as the iteration continues. This happens quickly at first and then gradually slows down as the algorithm finds better solutions that are more difficult to improve.

4. Numerical analysis

4.1 Numerical model

The effectiveness of the above methods for determining the structural dynamic reliability is demonstrated using a super large-scale Kiewitt (K6) single-layer lattice dome with welded joints. Some of the design parameters are taken from the literature [34]. The structure has a 300-metre span-length and a 45.21-metre height. It is made of seamless steel pipes with inner and outer radii of 0.4452 m and 0.4572 m, respectively. The structure has 331 welding connections and 930 members.

Using the OpenSeesPy program, a three-dimensional finite element model of the perfect dome is shown in Fig. 6. This paper, unlike previous studies, uses a parameterized modelling mode. Every steel pipe is divided into two displacement-based beam-column elements to model the initial imperfections. There are 1261 nodes and 1860 elements in the finite element model. The cross section of the steel pipe is dispersed into 20 and 3 fibres in the circumferential and radial directions, respectively. In this paper, the torsion effect of the cross section is considered. Steel fibres have a bilinear stress-strain material property. The uniform roof mass is concentrated to the nodes of the finite element model based on mass equivalence. The positions of certain members are marked in Fig. 6 for the output of the axial force.

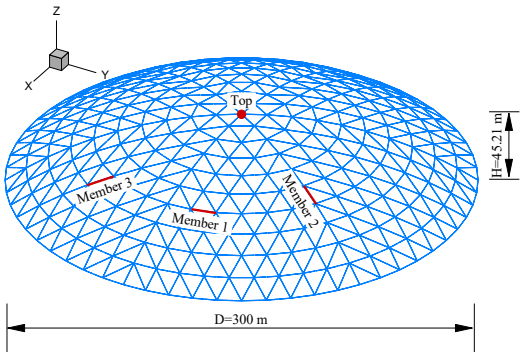

Fig. 6 Finite element model

4.2 Variables

Uncertain parameters are listed in Table 2. The stochastic variability of the low-level parameters, such as the elastic modulus, yield strength, and strain-hardening ratio of steel material, as well as the stochastic variability of the high-level parameters, such as the node error, member imperfection, wall-thickness of the steel pipes, node load (mass), structural damping ratio, and acceleration amplitudes of earthquake ground motions, are included in the structural reliability analysis. Uncertainties of ground motions are complex, and only the variability of acceleration amplitudes (aleatoric uncertainty) is taken into account in this paper. Most engineering variables obey truncated normal distributions according to the literature [35-42]. Thus, variable intervals can be described in the range of $\mu \pm c\sigma$, and the cases of $c = 1, 2, 3$ are discussed. Furthermore, these variables are assumed to be independent. Figs. 7-9 show the histograms, PDF curves, CDF curves, and fitted curves for the variables in Table 2, in which the sampling size is 320 and the constant c is equal to 3. The fitted curves are completely compatible with the real curves, and the sample size of 320 fully reflects the stochastic characteristics of the variables. Thus, the sample size of 320 is adequate for evaluating the variables.

Table 2 Variables for dynamic reliability analysis [35-42]

Level	Variable ($\boldsymbol{X}$)	Mean ($\boldsymbol{\mu}$)	Sd ($\boldsymbol{\sigma}$)	Bound	Distribution
Low-level uncertainties	Elastic modulus, E/Pa	μ=2.06e11	0.04× μ	$\{\mu - c\sigma, \mu + c\sigma\}$	$X_b \sim Norm(\mu, \sigma)$ (Truncated)
	Yield strength, f_y/Pa	$\mu = 235e6$	0.1× μ		
	Strain-hardening ratio, b	$\mu = 0.015$	0.2× μ		
High-level	Node error (x, y, or z), N_{err}/m	0	0.013		

uncertainties	Member imperfection (x, y, or z), M_{imp}/m	0	l/5196		
	Wall-thickness of the steel pipe, t_w/m	$\mu = 0.012$	0.067× μ		
	Node load, N_l/kg	$\mu = 10193.7$	0.1× μ		
	Damping ratio, ξ	$\mu = 0.02$	0.3× μ		
	Scale factor (earthquake), $\boldsymbol{S_f}$	$\boldsymbol{\mu}$=$\boldsymbol{g}$	0.1× $\boldsymbol{\mu}$		

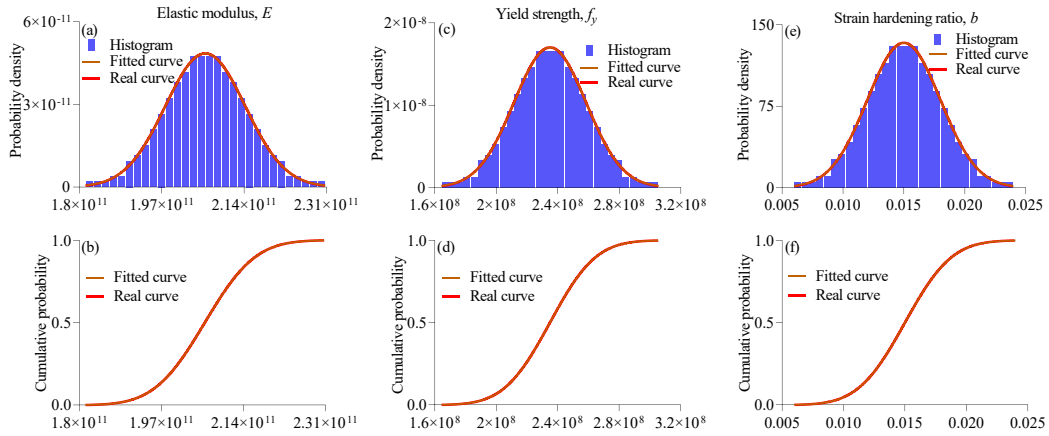

Fig. 7 Material parameters

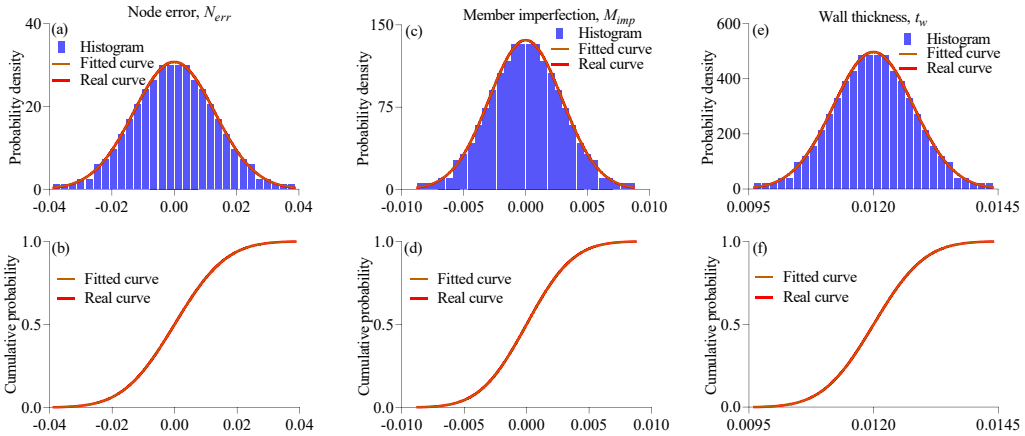

Fig. 8 Structural imperfections

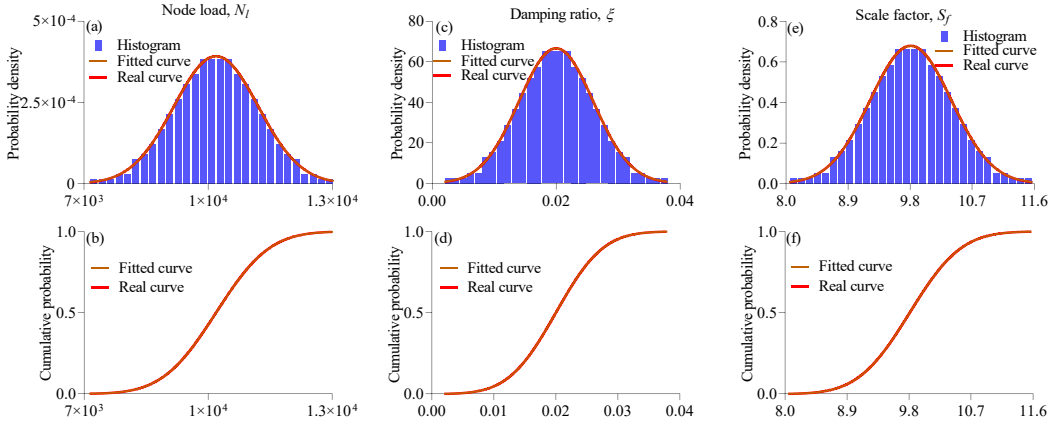

Fig. 9 Nodal mass, damping ratio, and scale factor

The damping ratio is the most discrete variable in Table 2. The effects of different sample sizes on stochastic properties are discussed in this paper based on this variable, as shown in Fig. 10. In the fitted PDF curves, the effects of the sample size on the stochastic and statistical properties are noticeable,

particularly in the extreme value regions. A sample size between 300 and 400 is considered to be the most appropriate since sample sizes greater than 300 have no effect on the stochastic and statistical properties.

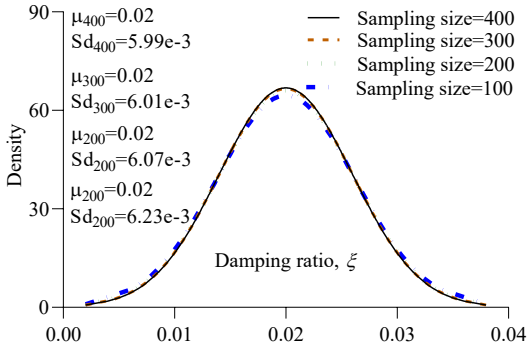

Fig. 10 Statistical properties under different sampling sizes

Because of the effect of uncertainty propagation in a structural system, the number of sample structures should be greater than that of the variables. The following is an empirical formula for the minimum number of samples [43],

$$N \approx {Z_{\alpha/2}}^2 Cov^2/h^2 \tag{10}$$

in which $Z_{\alpha/2}$ is the reliability coefficient; the values of $Z_{\alpha/2}$ are equal to 1.96 and 1.645, respectively, when the confidence levels are 95% and 90%; Cov is the variation coefficient; and h is the relative sampling error. The relative sampling error, as listed in Table 3, can be used to measure the sample size using Eq. (10). Table 3 shows that increasing confidence and coefficient of variation, as well as decreasing relative error, results in a larger sample size. In engineering, a confidence level of 95% is generally considered, and a relative error of less than 2% is appropriate.

Table 3 Relationship between the confidence level and the relative sampling error

Variation coefficient	Confidence level	Error				
		1%	2%	3%	4%	5%
0.3	95%	3457	864	384	216	138
	90%	2435	609	270	152	97
0.1	95%	384	96	43	24	15
	90%	271	68	30	17	11

4.3 Structural failure

The structural instability in single-layer domes denotes structural failure. Overall dynamic instability and local dynamic instability are two forms of dynamic instability. The concaveness in a particular region of the dome is referred to as a local instability. Local dynamic instability typically occurs before overall dynamic instability. The overall dynamic instability occurs as the area of local dynamic instability continues to expand, and the structure collapses. A single-layer dome is typically more vulnerable to buckling than a double-layer dome. As a consequence, the deformation can be used to monitor the dynamic instability of the dome. According to a Chinese industry standard [37], the maximum vertical deflection of a dome is limited to $1/n_D$ of its span-length; thus, the structural failure function $g(X)$ can be written as,

$$g(X) = {}^1/_{n_D} \times D - max\left\{d_{i,v,max} \middle|_{i=1}^{i=num}\right\} \tag{11}$$

where n_D is a constant, D is the span-length, $d_{i,v,max}$ is the maximum deformation in the time-history series of vertical displacement of the i^{th} connection in the $-Z$ direction, and num is

the number of connections within the structure. The value of n_D is approximately equal to 200 [44] when a perfect dome loses global stability. For a dome with variables, the value of n_D is large, and the different values of n_D are discussed for structural reliability analysis in this paper.

4.4 Earthquake ground motion

Three typical earthquake ground motion records are chosen as the external excitations of the dome from the PEER Strong Ground Motion Database. Table 3 lists the details of these ground motions, which represent minor, moderate, and major earthquakes applied to the structure according to their acceleration amplitudes. The acceleration peaks of these ground motions are considered to be uncertain, as discussed above and are adjusted according to the scale factors determined in Table 2.

Table 3 Earthquake ground motion records.

No.	Event	Station	Year	PGA/(g)			Duration/s
				x	y	z	
1	Imperial Valley-06	Calipatria Fire Station	10/15/1979	0.129	0.079	0.056	38
2	Imperial Valley-06	Chihuahua	10/15/1979	0.27	0.254	0.216	50
3	Northridge-01	Newhall - Fire Station	1/17/1994	0.566	0.590	0.548	40

4.5 Computational procedure of SFEM

Fig. 11 shows a universal flowchart for steel structures subjected to a single group of earthquake ground motions to better understand the core computational framework for structural reliability analysis. A group of variables in Table 2 are first generated using the LHS method based on the sampling size and number of variables during the computational process. The finite element model of a perfect dome is modified using the i^{th} group of variable arrays for the i^{th} sample structure until all the uncertain structures are evaluated. The GA is used to perform regression analysis on the PDF of structural demand, and then, the stochastic and statistical characteristics of the structural failure function are predicted.

The computational program for SFEM is completely coded in the OpenSeesPy framework based on the Python programming language. The SFEM in this paper can be extended to include almost all potentially uncertain variables with probabilistic properties.

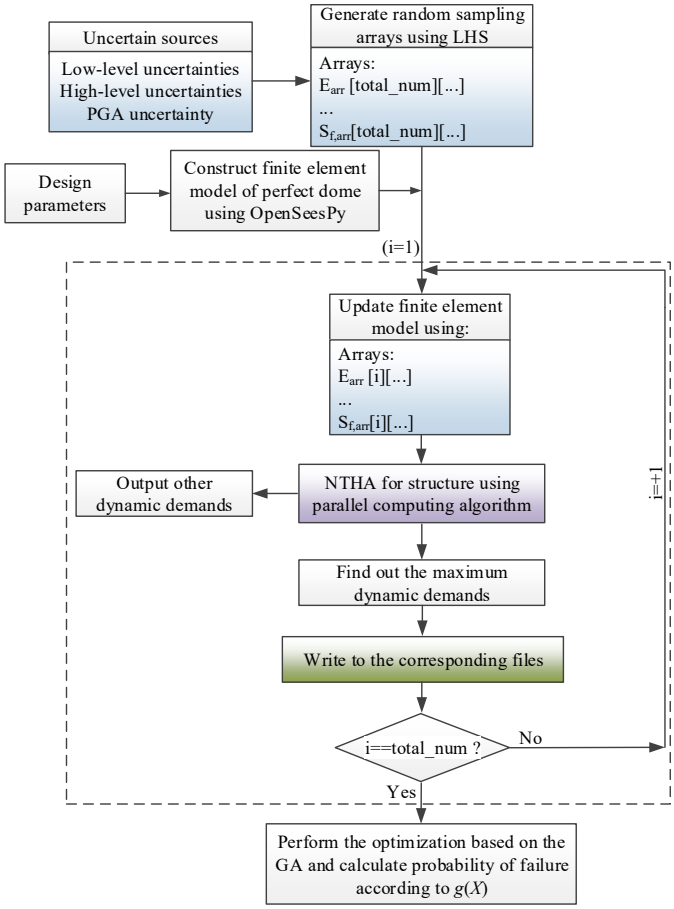

Fig. 11 Computational procedure for SFEM for each ground motion

4.6 Parallel computing

Although advanced sampling techniques have been used to calculate the dynamic reliability of large-scale complex engineering structures, computing is still time-consuming. To improve computing efficiency, parallel processing is a commonly used mode of operation, and tasks are performed in multiple processors on the same computer at the same time. In Python, the multiprocessing module runs parallel processes independently using child processes instead of threads. Because multiple processors can be used on a single computer, processes can run in completely separate memory locations. In multiprocessing, there are two main modes for parallel execution: the pool mode and the process mode. A time-consumption comparison suggests that the pool mode is the mode best suited for parallel computing in this paper. Using a standard desktop computer with 16 CPUs, it takes only 8.36 hours per 1000 sampling structures under one earthquake record according to a test.

5. Results and discussion

5.1 Sample stability for results

The improved LHS method is used in this paper to reduce the sampling size to accelerate the computational process. Although the sampling size of 320 is adequate to analyse the variables in Table 2, it can only ensure that the value of a variable (x_i or x_j) is not repeatedly selected in the interval. However, the uncertainty propagation is nonlinear due to the effect of the combination of multiple variables on structural dynamic demands in SFEM, which means that the combination of stochastic values of different variables may lead to the same structural demand values. This leads to the aggregation of structural demand values in dynamic analyses. To avoid this, the number of sampling structures in this paper was increased considerably; a sample size of 1000 is used in a single analysis.

Although the determination of the sample size required for the reliability studies is subjective, the rationality of the sample size can be confirmed by the convergence of results in structural analyses. The sensitivity of the mean values and the standard deviations of the dynamic demands to sample size is shown in Fig. 12. Here, an unfavourable case under the Northridge-01 earthquake and c=3 is used to validate the reliability of the results, as the PGAs in this earthquake are the largest and c=3 reflects the widest range of variable values. It can be seen from the figure that hundreds of samples lead to unstable results. As the sample size increases, the results gradually stabilize to their mean values. When the sample size reaches 1000, the results are stable.

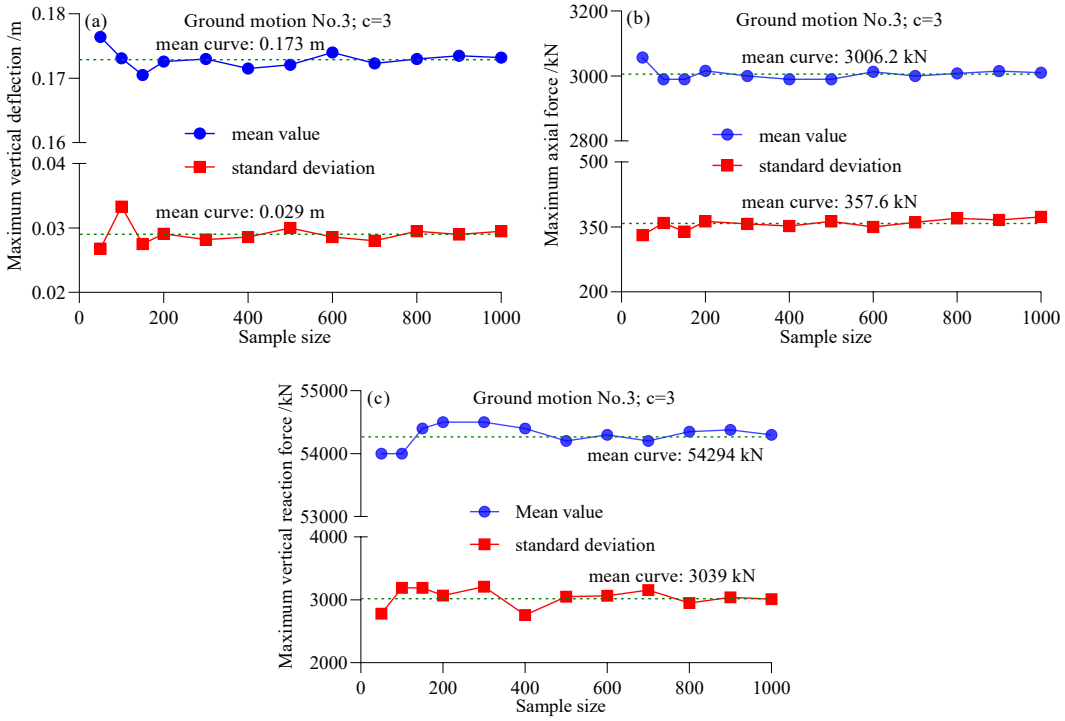

Fig. 12 Convergence of results

5.2 Dynamic demands

5.2.1 Statistical characteristics of the dynamic demands

When a structural probability analysis is carried out, the structural demands experience intervals since the different variable values lead to different structural demands, while the structural demands in the deterministic methods are constant. Fig. 13 shows the statistical histograms of the maximum dynamic demands and the values of the deterministic dynamic demands for two earthquake records. Fig. 13(a) shows the peak displacement at the top in the X, Y, and Z directions. The mean values of these dynamic demands are slightly larger than those of the perfect dome. However, the mean values of the peak axial force in members 1, 2, and 3, which represent the diagonal member, hoop member, and ridge member, are less than the values of the axial force in the perfect dome, as shown in Fig. 13(b). Obviously, the uncertain variables in the structure lead to an increase in deformation and a decrease in bearing capacity, and the coefficients of variation (COVs) of these dynamic demands are approximately 10%-15%.

The estimated distribution interval of the structural demands describes the effect of variable uncertainties on the structural system. An index u_q is defined to further quantify the uncertainty of the results,

$$u_q = \frac{v_{max} - v_{min}}{\mu'} \tag{12}$$

where v_{max} and v_{min} are the maximum and minimum values of the structural demands at an interval, respectively, and μ' is the mean value of the structure demands. According to Eq. (12), a high value of u_q leads to a significant uncertainty in the results. From the estimated results in the figure, in displacement, the values of u_q are 0.89, 0.91, and 0.84 for the maximum displacements at the top in the X, Y, and Z directions, respectively. In terms of the axial force, the values of u_q are 0.82, 0.85, and 0.88 for members 1, 2, and 3, respectively. Generally, the variables in Table 2 have a more significant effect on the deformations than on the axial forces of the members.

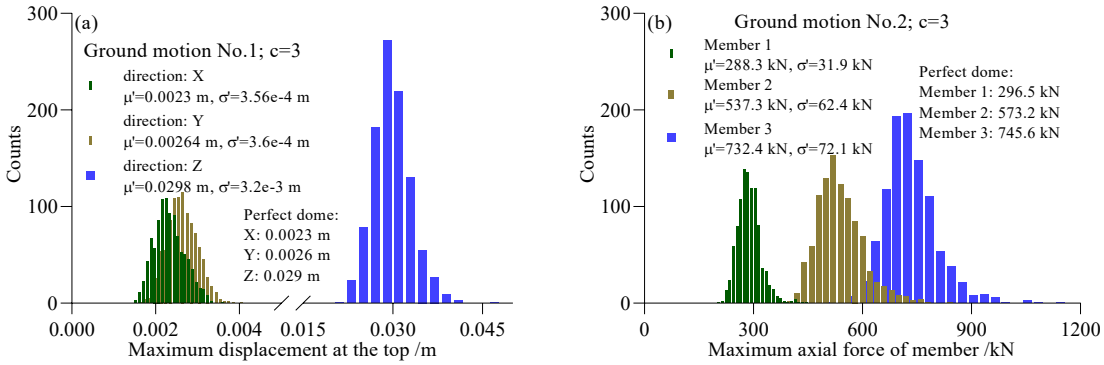

Fig. 13 Statistical histograms of maximum dynamic demands

5.2.2 Maximum vertical deflection in the dome

The evaluation of various statistical parameters, such as the probability distribution intervals of the maximum vertical deflection of the dome, plays an important role in reliability analysis. Based on the SFEM, the PDFs and CDFs of the maximum vertical deflections of 1000 sample structures under ground motion No. 1 (Imperial Valley-06, Calipatria Fire Station) and c=1, 2, and 3 are shown in Fig. 14, and the fitting statistical parameters for the PDFs are listed in Table 4. Here, two methods are compared: PDFs and CDFs obtained using the GEV model and the GA+GEV model. It is observed that the interval range of structural demand increases with the increase in the scale factor c, particularly for the upper bound, while the lower bound is almost unaffected by the scale factor. The COVs for the scale factors c=1, 2, and 3 are approximately 4.3%, 5.7%, and 6.1%, respectively, and the difference for the PDFs or CDFs decreases with the increase in the scale factor. The scale factor c should be chosen carefully, as shown in Fig. 14(b), since the small values of the scale factor may lead to an overestimation of the reliability of the dome. According to Table 4, it is observed that the values of Q^2 are greater than 0.9, indicating excellent robustness of the two methods for PDFs, while the GA optimization improves the fitting precision of PDFs obtained only through the GEV model. Particularly for the case of c=3, the PDFs and CDFs are clearly improved. The observed values and predicted values for PDFs are plotted in Fig. 15. Both models have a high degree of goodness-of-fit.

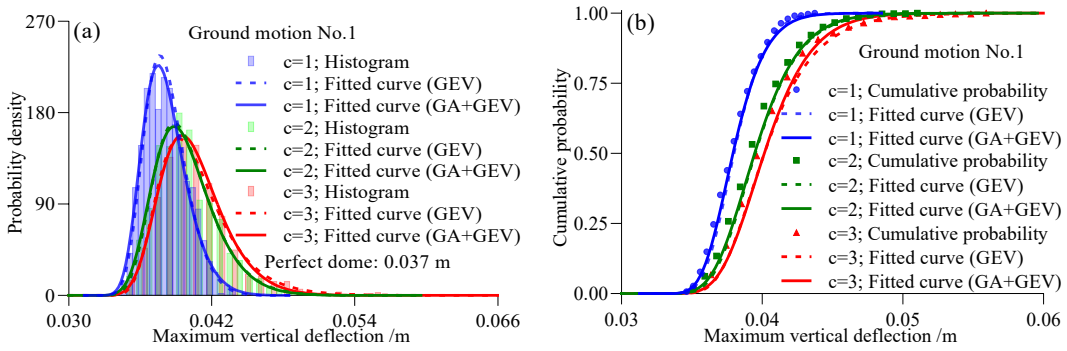

Fig. 14 PDFs and CDFs of maximum vertical deflection

Table 4 Fitting values of unknown variables for PDFs of the maximum vertical deflection.

Method	c=1				c=2				c=3			
	k	δ/m	mu/m	Q^2	k	δ/m	mu/m	Q^2	k	δ/m	mu/m	Q^2
GEV	-0.1278	1.6e-3	0.0374	*0.94*	-0.0564	0.0022	0.0387	*0.97*	-0.0619	0.0024	0.0393	*0.97*
GA+GEV	-0.0847	1.6e-3	0.0374	*0.96*	-0.0787	0.0022	0.0387	*0.97*	-0.08	0.0023	0.0393	*0.99*

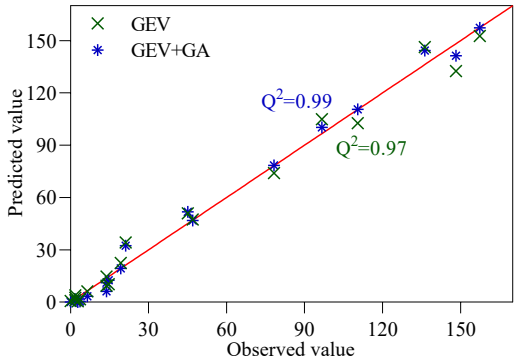

Fig. 15 Validation for optimizing the PDF

5.2.3 Maximum axial force of the dome

The members of the dome are primarily subjected to axial forces. The maximum axial force in all members varies in each SFEM analysis. The maximum values of the axial force, including compression and tension, are statistically evaluated in this paper. The PDFs and CDFs of the maximum axial force in the dome under ground motion No. 2 (Imperial Valley-06, Chihuahua) and c=1, 2, and 3 are shown in Fig. 16. The fitting parameters for PDFs with the GEV model and the GA+GEV model are listed in Table 5. With the increase in the scale factor c, the maximum axial force varies considerably, and the distribution interval increases significantly. The COVs are approximately 4%, 6.5%, and 7.6% for the scale factors c=1, 2, and 3, respectively. However, the change in the mean values (the location parameter) of the maximum axial force is not obvious. According to Table 5, the GA can further optimize the shape parameter k and find the optimal location mu and scale parameter δ; as a result, the GA optimization increases the fitting precision of the GEV model and improves the performance of SPA.

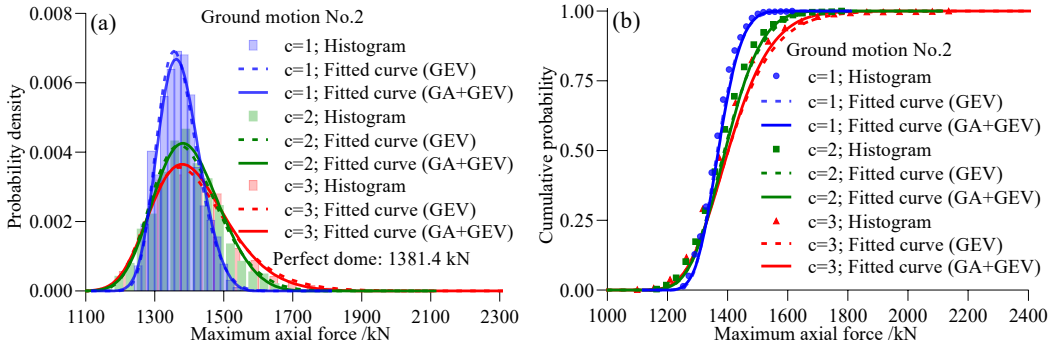

Fig. 16 PDFs and CDFs of the maximum axial force

Table 5 Fitting values of unknown variables for the maximum axial force.

Method	c=1				c=2				c=3			
	k	δ/kN	mu/kN	Q^2	k	δ/kN	mu/kN	Q^2	k	δ/kN	mu/kN	Q^2
GEV	-0.1605	53.99	1.347e3	*0.96*	-0.1498	88.55	1.358e3	*0.97*	-0.0642	103.44	1.365e3	*0.97*
GA+G	-0.2127	56.38	1.349e3	*0.97*	-0.2122	88.51	1.361e3	*0.99*	-0.1320	101.53	1.366e3	*0.99*

5.2.4 Maximum total vertical reaction force (MTVRF) at supports

The vertical reaction force at the supports, which has been investigated in previous literature because it reflects the structural bearing capacity, is one of several important mechanical parameters of the dome. The MTVRF is found in this paper by extracting and summing the time-history data for the vertical reaction force at 60 supports. Following that, as shown in Fig. 17, the values of the MTVRF for 1000 sampling structures under ground motion No. 3 (Northridge-01) and c=1, 2, and 3 are statistically analysed. With the increase in the scale factor c, the values of the MTVRF vary within a wider interval, although their mean values are nearly identical and close to the values in the deterministic analysis. Their CDFs for scale factors c=2 and 3 are very similar. For scale factors c=1, 2, and 3, the COVs are approximately 3.4%, 5.1%, and 5.4%, respectively. Table 6 lists the PDFs' parameters that are fitted. Clearly, the GA further increases the fitting precision of the PDFs.

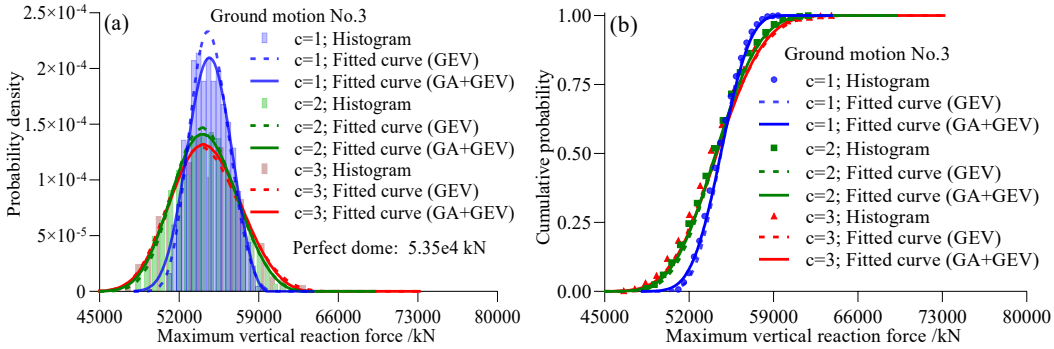

Fig. 17 PDFs and CDFs of MTVRF at supports

Table 6 Fitting values of unknown variables for MTVRF at supports.

Method	c=1				c=2				c=3			
	k	δ/kN	mu/kN	Q^2	k	δ/kN	mu/kN	Q^2	k	δ/kN	mu/kN	Q^2
GEV	-0.2472	1.63e3	5.4e4	*0.94*	-0.2404	2.59e3	5.3e4	*0.97*	-0.2277	2.9e3	5.3e4	*0.96*
GA+GEV	-0.3182	1.86e3	5.4e4	*0.97*	-0.2675	2.71e3	5.3e4	*0.99*	-0.2627	2.9e3	5.3e4	*0.97*

5.3 Structural reliability analysis

The CDFs of the maximum vertical deflection under different earthquakes and interval parameters can be obtained based on the GA+GEV model with a high precision, as shown in Fig. 18. Table 7 lists the fitting parameters. From the figure, the constant c has a major influence on the CDFs and the intervals of variables should be carefully considered. The structural reliability under an earthquake usually decreases as the constant c increases. The cumulative probabilities of the maximum vertical deflection are given by these CDFs. The structural reliability P_s can be calculated using the fitted parameters and Eq. (6) when a displacement threshold is defined.

The goal of structural reliability is to develop design criteria and verification procedures that ensure that structures designed according to specifications can perform as expected in terms of safety and serviceability. In structural reliability analysis, the aim is to calculate the probability of failure, where failure is defined as a violation of the limit state function, as expressed in Eq. (11). The following is a formula for the relationship between structural reliability and failure probability,

$$P_f = 1 - P_s \tag{13}$$

Table 8 lists the failure probability and corresponding structural reliability index β under the earthquake Northridge-01 and c=3 according to the parameters in Table 7 and Eq. (13). The FOSM method and the current method are compared. The different values of n_D in Eq. (11) are discussed. The results show that the probabilities of failure are low under this earthquake, and the structure has

high dynamic reliability index values. Compared with the current method, the FOSM leads to a higher structural reliability, which overestimates the structural safety.

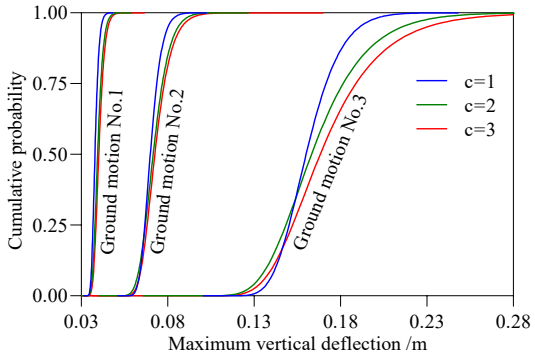

Fig. 18 CDFs of maximum vertical deflection under three earthquakes

Table 7 Fitting values of unknown variables under different earthquakes.

Earthquake	***c*=1**			***c*=2**			***c*=3**		
	k	δ/m	mu/m	k	δ/m	mu/m	k	δ/m	mu/m
Ground motion No. 1	-0.0847	0.0016	0.0374	-0.0787	0.0022	0.0387	-0.08	0.0023	0.0393
Ground motion No. 2	-0.1015	0.0042	0.0684	-0.0985	0.0065	0.0693	-0.0493	0.0065	0.0702
Ground motion No. 3	-0.1118	0.0143	0.155	-0.0212	0.0202	0.1569	0.0147	0.0231	0.1598

Table 8 Probability of structural failure and reliability index (c=3).

Parameters	n_D=600	n_D=400	n_D=300
P_f (Current study)	1.623e-6	3.782e-10	2.2e-13
β (Current study)	4.65	6.15	7.24
β (FOSM)	11.08	19.56	28.04
P_f (FOSM)	7.8e-29	1.7e-85	2.6e-173

5.4 Sensitivity of estimated dynamic reliability parameters to sample size

The value of the probability of failure obtained from the sampling methods is found to be sensitive to the sample size [28]. The effect of sample size on the estimated dynamic reliability parameters is discussed in this paper using the Northridge-01 earthquake and c=3. Here, n_D is set to 600. Fig. 19 shows the failure probabilities and the corresponding reliability indices for different sampling sizes. The sample size has a significant effect on the estimated dynamic reliability parameters, as shown; hundreds of samples can result in a high probability of failure and a low reliability index. The values of the reliability index begin to converge after the sample size reaches 400. Therefore, a larger sampling size is needed for higher calculation precision of failure probability.

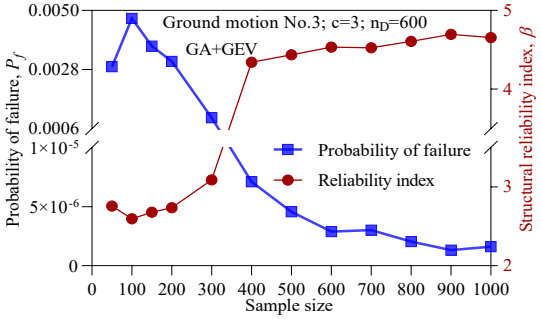

Fig. 19 Probability of failure and structural reliability index

6. Effects of variables on structural performance

The effects of variables on the structural performance need to be investigated for a comprehensive reliability analysis to determine the variables that have the greatest effect on structural performance.

Using the Northridge-01 earthquake and c=3, the following results are obtained. Here, the effect of variables on structural dynamic performance is assessed using three different methods. Because the values of the variables in each member are unique, the following analyses are different from traditional sensitivity analyses except for the structural damping ratio. Here, each analysis for each variable is based on 1000 sample structures.

6.1 Effect of variables on structural performance based on COV

According to the analyses in Sections 5.2 and 5.3, changing the value of a variable causes a variation in dynamic demands, and a large variation interval of dynamic demand values indicates a large effect of the variable on structure performance. As stated in the literature [45], the standard deviation of the results is a measure of the uncertainty for a variable. Therefore, COV is defined to evaluate the effect,

$$S_i = std(d_i)/mean(d_i) \tag{14}$$

where $std(d_i)$ refers to the standard deviation of the maximum vertical deflection d_i in the dome caused by the i^{th} variable, and $mean(d_i)$ represents the mean value of d_i. A large standard deviation means that structural demands can vary significantly from the mean value. Therefore, the larger the value of S_i is, the greater the effect of the variable on the structure. The normalized value of S_i is determined using 1000 sampling structures for each variable, as shown in Fig. 20. The damping ratio ξ, roof load N_l, scale factor of ground motion S_f, and wall-thickness of the steel pipe t_w are found to be the four most important variables that affect the interval of the dynamic demand. The parameters of the steel material f_y and b have the least effect on the structure.

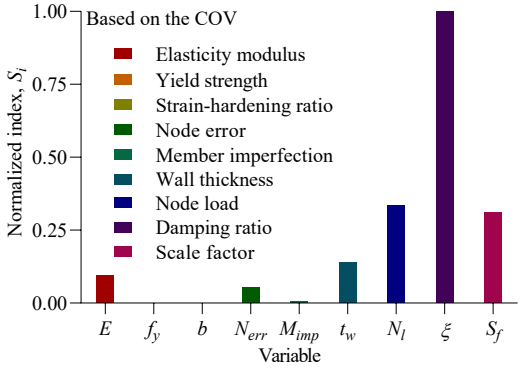

Fig. 20 Effect of variables on maximum vertical deflection

6.2 Effect of variables on the structural performance based on the probability of failure P_f

Calculations based on P_f typically yield valuable information about the effect of random variables on the structural performance. The importance of the effect of variables on structural performance is assessed. To increase the identification accuracy, the parameter n_D is set to 1000. Based on the maximum vertical deflection, Fig. 21 shows the structural probability of failure induced by each variable. The roof load N_l, damping ratio ξ, scale factor of ground motion S_f, and wall-thickness of the steel pipe t_w are the four most important variables that affect the structural failure probability. The parameters of the steel material f_y and b, node error N_{err}, and member imperfection M_{imp} have the least effect on the structure.

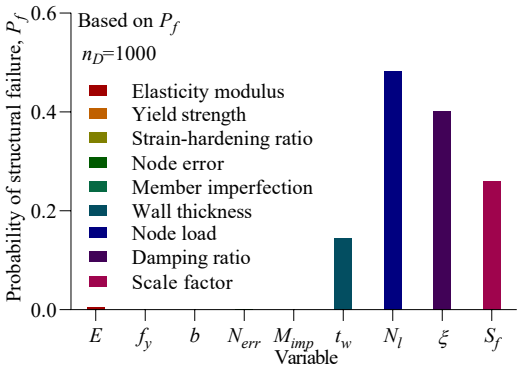

Fig. 21 Effect of variables on probability of failure

6.3 Effect of variables on structural performance based on the index u_q

Eq. (12) reflects the effect of a variable on the structural demands. This index u_q is used to investigate the effect of variables on the maximum vertical deflection of the dome in this section. Fig. 22 shows the value of the normalized index for each variable. It is observed that there is only a slight difference between the evaluation based on the COV in Section 6.1 and the evaluation based on the index u_q. The damping ratio ξ, roof load N_l, scale factor of ground motion S_f, and wall-thickness of the steel pipe t_w are the four most important variables in the dome with variables.

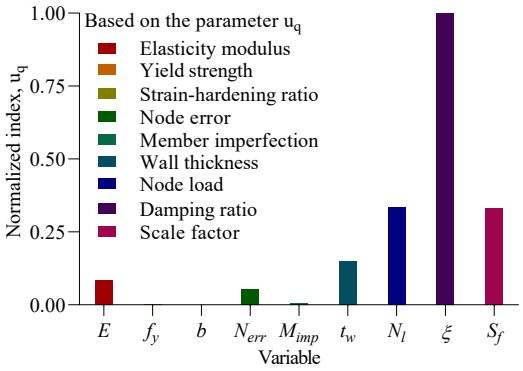

Fig. 22 Effect of variables on the structural demands using the index μ_q

6.4 Discussion

From the above analysis, the effect of different variables on the structural performance is varied with the evaluation method. The damping ratio, external excitation, and roof load are the three most important variables in structural dynamic analysis, and these variables should be carefully considered. There are several approaches to improve structural performance and increase the reliability of the dome under uncertain conditions:

- Change the mean values of important variables, e.g., appropriately increase or decrease the mean values of variables that are favourable or unfavourable for structural reliability.
- Reduce the variance of variables, e.g., reduce all types of errors.
- Reduce the variation intervals of important variables, e.g., improve quality control in the construction process.

7. Conclusions

The new SFEM method for solving structural dynamic reliability using the NTHA has been developed and the results show its effectiveness and high accuracy for super large structures. The computational performance has been boosted by integrating the highly efficient LHS sampling process, GA for optimization, and parallel computing. The uncertain quantification per 1000 super large-scale domes only takes less than 10 hours on a standard desktop computer. It largely expands the spatial scale

of the structure and computational capability in dynamic reliability problems.

Considering that the uncertainties lead to an increase in the mean values of deformation demands and a reduction in the mean values of axial force in members compared to the perfect dome, these maximum dynamic demands have a COV of approximately 4%-8% in sample structures. There is no obvious change in the mean values of MTVRF. However, the MTVRF has a COV of approximately 3%-5.5% in sample structures. Compared with the GEV model, GA optimization can further improve the PDFs and CDFs of structural demands. It is also found that as the intervals of variables become wider, the structural reliability decreases. When calculating the probabilities of failure, the FOSM method overestimates the structural safety compared with the current method. The damping ratio ξ, roof load N_l, scale factor of ground motion S_f, and wall-thickness of the steel pipe t_w are the four most important variables of the dome according to an investigation of the effects of variables on the structural performance.

Acknowledgements

We would like to acknowledge the financial support from the National Key Research and Development Program of China (Grant No. 2018YFC1504304), Key Project of the Natural Science Foundation of Tianjin City (Grant No. 19JCZDJC39300), and National Natural Science Foundation of China (Grant No. 51878433).

References:

[1] Vamvatsikos D and Fragiadakis M. Incremental dynamic analysis for estimating seismic performance sensitivity and uncertainty. Earthquake Engineering & Structural Dynamics 2010; 39(2): 141-163.

[2] Bradley BA. A critical examination of seismic response uncertainty analysis in earthquake engineering. Earthquake Engineering & Structural Dynamics 2013; 42(11): 1717-1729.

[3] Der Kiureghian A. Analysis of structural reliability under parameter uncertainties. Probabilistic Eng Mech 2008; 23: 351-358.

[4] Valdebenito MA, Labarca AA, Jensen HA. On the application of intervening variables for stochastic finite element analysis. Computers & Structures 2013; 126: 164-176.

[5] Smith AP, Garloff J and Horst W. Verified solution for a statically determinate truss structure with uncertain node locations. Journal of Civil Engineering and Architecture 2010; 4(11): 1-10.

[6] Cruse TA, Wu YT, Dias B, Rajagopal KR. Probabilistic structural analysis methods and applications. Computers & Structures 1988; 30(1-2): 163-170.

[7] Bulleit WM. Uncertainty in structural engineering. Practice Periodical on Structural Design and Construction 2008; 13(1): 24-30.

[8] Matthies HG, Brenner CE, Bucher CG, et al. Uncertainties in probabilistic numerical analysis of structures and solids-Stochastic finite elements. Structural Safety 1997; 19(3): 283-336.

[9] Haukaas T, Scott MH. Shape sensitivities in the reliability analysis of nonlinear frame structures. Comput and Struct 2006; 84(15-16): 964-977.

[10] Zhang H, Mullen RL, Muhanna RL. Interval Monte Carlo methods for structural reliability. Structural Safety 2010; 32(3): 183-190.

[11] Zhang H, Dai H, Beer M, et al. Structural reliability analysis on the basis of small samples: an interval quasi-Monte Carlo method. Mechanical Systems and Signal Processing 2013; 37(1-2): 137-151.

[12] Le JL, Xue B. Probabilistic analysis of reinforced concrete frame structures against progressive collapse. Engineering Structures 2014; 76: 313-323.

[13] Liel AB, Haselton CB, et al. Incorporating modeling uncertainties in the assessment of seismic collapse risk of buildings. Structural Safety, 2009, 31(2): 197-211.

[14] Mitseas IP, Beer M. Fragility analysis of nonproportionally damped inelastic MDOF structural systems exposed to stochastic seismic excitation. Computers & Structures 2020; 226: 106129.

[15] McGill WL, Ayyub BM. Estimating parameter distributions in structural reliability assessment using the Transferable Belief Model. Computers & Structures 2008; 86(10): 1052-1060.

[16] Graf W, Goetz M, Kaliske, M. Analysis of dynamic processes under consideration of polymorphic uncertainty. Structural safety, 2015, 52:194-201.

[17] Zhang HD, Zhu XQ, Yao S. Nonlinear dynamic analysis method for large-scale single-layer lattice domes with uncertain-but-bounded parameters. Engineering Structures 2020; 203: 109780.

[18] Zhang L, Zhang J, You L, et al. Reliability analysis of structures based on a probability-uncertainty hybrid model. Quality and Reliability Engineering 2019; 35(1):263-279. https://doi.org/10.1002/qre.2396

[19] Jiang C, Li WX, Han X, et al. Structural reliability analysis based on random distributions with interval parameters. Computers & Structures 2011; 89(23-24): 2292-2302.

[20] Králik J. Probability and sensitivity analysis of soil-structure interaction of high-rise buildings. Slovak Journal of Civil Engineering 2006; 5(3): 18-32.

[21] Hariri-Ardebilia MA, Sudret B. Polynomial chaos expansion for uncertainty quantification of dam engineering problems. Engineering Structures 2020; 203: 109631.

[22] Wang YZ, Zheng XY, Cheng L, et al. Structural dynamic probabilistic evaluation using a surrogate model and genetic algorithm. Proceedings of the Institution of Civil Engineers - Maritime Engineering 2020; 173(1): 13-27. https://doi.org/10.1680/jmaen.2019.28

[23] Cui L, Sheng D. Genetic algorithms in probabilistic finite element analysis of geotechnical problems. Computers and Geotechnics 2005; 32: 555-563.

[24] Cheng J, Li QS, et al. A new artificial neural network-based response surface method for structural reliability analysis. Probabilistic Eng Mech 2008; 23(1): 51-63. doi:10.1016/j.probengmech.2007.10.003

[25] de Santana Gomes WJ. Structural reliability analysis using adaptive artificial neural networks. ASCE-ASME Journal of Risk and Uncertainty in Engineering Systems Part B: Mechanical Engineering 2019; 5(4): 041004. doi:10.1115/1.4044040

[26] Melchers RE. Assessment of existing structures-approaches and research needs. Journal of Structural Engineering (ASCE) 2001; 127(4): 406-411.

[27] Schuëller GI, Pradlwarter HJ. Uncertain linear systems in dynamics: Retrospective and recent developments by stochastic approaches. Engineering Structures 2009; 31: 2507-2517.

[28] Olsson A, Sandberg G, Dahlblom O. On Latin hypercube sampling for structural reliability analysis. Structural Safety 2003; 25(1):47-68. https://doi.org/10.1016/S0167-4730(02)00039-5

[29] Nascimento F, Bourguignon M, Leao J. Extended generalized extreme value distribution with applications in environmental data. Hacettepe Journal Of Mathematics And Statistics 2016; 45(6):1847-1864.

[30] Raggad B. Stationary and non-stationary extreme value approaches for modelling extreme temperature: the Case of Riyadh City, Saudi Arabia. Environmental Modeling & Assessment 2018; 23(1): 99-116.

[31] Pinheiro EC, Ferrari SLP. A comparative review of generalizations of the Gumbel extreme value distribution with an application to wind speed data. J Stat Comput Simul 2016; 86(11): 2241-2261.

[32] Jahani E, Shayanfar MA, Barkhordari MA. Structural reliability based on genetic algorithm - Monte Carlo (GAMC). Advances in Structural Engineering 2013; 16(2): 419-426. doi:10.1260/1369-4332.16.2.419

[33] Schüürmann G, Ebert RU, Chen J, et al. External validation and prediction employing the predictive squared correlation coefficient - Test Set Activity Mean vs Training Set Activity Mean. J. Chem. Inf. Model. 2008; 48(11): 2140-2145. doi:10.1021/ci800253u

[34] Choi D, Park K. The time history analysis of 300m single-layer lattice domes. International Journal of Innovations in Engineering and Technology (IJIET) 2019; 13(2): 32-36. http://dx.doi.org/10.21172/ijiet.132.06

[35] Motra HB, Hildebrand J, Dimmig-Osburg A. Assessment of strain measurement techniques to characterise mechanical properties of structural steel. Engineering Science and Technology, an International Journal 2014; 17(4): 260-269. doi:10.1016/j.jestch.2014.07.006

[36] Sadowski AJ, Michael RJ, Reinke T, Ummenhofer T. Statistical analysis of the material properties of selected structural carbon steels. Structural Safety 2015; 53: 26-35.

[37] Industry standard of the People's Republic of China. JGJ7-2010: Technical specification for space frame structures. Ministry of Housing and Urban-Rural Development, China, 2010. <http://www.gbstandards.org/GB_standard_english.asp?code=JGJ%207-2010&word=Technical%20specification%20for%20sp>

[38] Liu XC, Zhang AL, Ge JQ, Wang L, Qi ZL. Study on the influence of construction deviation random distribution on the integral stability of suspend-dome. Journal of Building Structures 2007; 28(6): 76-82. http://manu25.magtech.com.cn/Jwk3_jzjgxb/CN/

[39] Mateus AF, Witz JA. Collapse of imperfect corroded steel tubes. In: 22nd International Conference on Offshore Mechanics and Arctic Engineering, ASME, 2003; pp. 217-225. https://doi.org/10.1115/OMAE2003-37123

[40] Mohammadi J , Modares M. Practical approach to using uncertainties in structural condition assessment. Practice Periodical on Structural Design and Construction 2013; 18(3): 155-164. https://doi.org/10.1061/(ASCE)SC.1943-5576.0000149

[41] Fiore A, Greco R. Influence of structural damping uncertainty on damping reduction factor. Journal of Earthquake Engineering 2020; 1-22. DOI:10.1080/13632469.2020.1747573

[42] Bakhshi A, Asadi P. Probabilistic evaluation of seismic design parameters of RC frames based on fragility curves. Scientia Iranica 2013; 20(2): 231-241.

[43] NIST/SEMATECH e-Handbook of Statistical Methods. http://www.itl.nist.gov/div898/handbook/. Department of Commerce, U.S, 2003. https://doi.org/10.18434/M321892003

[44] Guo H, Qian H, Shen S. Dynamic stability of single-layer reticulated domes under earthquake excitation. Earthquake Engineering and Engineering Vibration 2003; 23(1): 31-37. (in Chinese)

[45] Liu WL, Wu XG, Zhang LM, et al. Structural health-monitoring and assessment in tunnels: Hybrid Simulation Approach. J Perform Constr Facil 2020; 34 (4): 04020045. https://doi.org/10.1061/(asce)cf.1943-5509.0001445.